# ITERATIVE FILTERING BASED ON ADAPTIVE CHEBYSHEV KERNEL FUNCTIONS FOR NOISE SUPPRESSION IN DIFFERENTIAL SAR INTERFEROGRAMS

*Alejandro Mestre-Quereda, Juan M Lopez-Sanchez, Jesus Selva[1] and Pablo J. Gonzalez[2]*

[1]Signals, Systems and Telecommunications Group, IUII, University of Alicante, Spain.
[2]COMET, Dept. of Earth, Ocean and Environmental Sciences, University of Liverpool, United Kingdom.

## ABSTRACT

Differential SAR Interferometry (DInSAR) is a powerful remote sensing technique employed to monitor surface displacements, such as ground subsidence or strong deformations caused by geological activity. The quality of the interferometric phase between two combined SAR images is essential for the estimation of the surface deformation. Multiple decorrelation factors may degrade the quality of the measurements and, then, the development of filtering methods for noise suppression is mandatory. In this work, we propose a new strategy to improve noise reduction while preserving the original phase structure. The new method consists in an iterative filter in which noise reduction is achieved progressively. The original phase is filtered with adaptive kernels based on Chebyshev interpolation functions. The filter is especially useful for DInSAR geophysical applications, such as earthquakes or volcanic eruptions monitoring. The performance of the proposed method has been tested with both simulated data and recently acquired Sentinel-1 SAR data which mapped the August 2016 Central Italy earthquake.

## 1. INTRODUCTION

Geophysical phenomena, such as volcanic eruptions or seismic events, have been successfully monitored with the processing of interferometric SAR products. The quality of the interferometric phase, obtained from the combination of two co-registered Single-Look Complex (SLC) SAR images, constitutes the key element for the analysis of the Earth's surface deformation with Differential SAR Interferometry (DInSAR) [1, 2, 3]. Nevertheless, multiple sources of noise, including temporal decorrelation, geometrical or baseline decorrelation may be present in the observations and may degrade the accuracy of the estimations [4]. Consequently, signal processing techniques for interferometric phase images denoising are necessary.

In geophysical applications, the well-known Goldstein filter [5] is the most commonly used due to its general good performance and computational efficiency. According to [5], the original interferogram is divided into overlapped windows of a fixed size, and the 2-D Fourier Transform of the window is multiplied by its smoothed absolute value. The smoothing operation is achieved by means of a pre-defined convolution kernel. In addition, the filtering capability is controlled by an arbitrarily selected real parameter (usually denoted as $\alpha$) which value varies between 0 and 1. Higher values of $\alpha$ provide a stronger filtering and a higher noise reduction, at the cost of a resolution loss.

Different modifications of the original filter have been developed over the last years. An $\alpha$-adaptive Goldstein filter was proposed in [6]. In this case, the values of the filtering parameter $\alpha$ are selected as a function of the mean coherence of the filtering window, which is an indicator of the phase quality. Then, low-coherent areas will be filtered with higher values of $\alpha$, while resolution will be preserved in high-quality areas. A pixel-by-pixel filter was proposed in [7]. That is, instead of performing a block-based filter, every pixel in the phase image is individually filtered with adaptive windows. The filter shows very good results in fringe preservation, but noise reduction is not enough in noisy areas. Alternatively, an iterative filter named Recursive Adaptive Spectral Filter (RASF) was proposed in [8]. Unlike the previous filters, the RASF strategy shows very good results in noise suppression, even with very noisy scenes, but detailed features of the phase image are more likely to be overfiltered and fringe continuity may not be preserved.

In this work, we present a new interferogram filter which relies on the iterative and adaptive Goldstein approach, but it includes multiple modifications to improve its performance. The main objective of this new method is to effectively suppress the phase noise while preserving the original phase structure without overfiltering.

This work was supported by the Spanish Ministry of Economy, Industry and Competitiveness (MINECO), the State Agency of Research (AEI) and the European Funds for Regional Development (FEDER) under Projects TIN2014-55413-C2-2-P and TEC2017-85244-C2-1-P. This work was partially supported by the UK Natural Environmental Research Council (NERC) through the "Looking Inside the Continents (LiCS)" (NE/K011006/1), the "Rapid deployment of a seismic array in Ecuador following the April 16th 2016 M7.8 Pedernales earthquake" (NE/P008828/1), and the Centre for the Observation and Modelling of Earthquakes, Volcanoes and Tectonics (COMET, GA/13/M/031, http://comet.nerc.ac.uk) projects.

## 2. PROPOSED METHOD

### 2.1. Chebyshev Polynomials and Kernel Generation

The idea behind kernel generation is the mathematical approximation theory of a generic 2-D function $F$ by means of a set of polynomials. For simplicity, we assume that $F$ is defined in $[-1,1]\times[-1,1]$. In this case, we propose the use of a generic sum of a set of Chebyshev polynomials. Thus, we assume that $F$ can be well approximated as

$$F(x,y) \approx \sum_{k=0}^{K_x-1}{}' \sum_{r=0}^{K_y-1}{}' c_{k,r} T_k(x) T_r(y), \tag{1}$$

where the prime (') indicates that the $k=0$ summand must be multiplied by $1/2$, $c_{k,r}$ is the set of unknown coefficients that we want to estimate and that correspond to kernel values, and $T_k(z)$ is the Chebyshev polynomial of the first kind and order $k$. The standard definition of such a polynomial is

$$T_k(z) \equiv \cos(k \arccos z), \qquad z \in [-1,1] \tag{2}$$

Next, we assume that $F$ is sampled within a regular grid in $[-1,1]\times[-1,1]$ at abcissas $x_p$, $y_p$. For simplicity, the grid is assumed to be squared and its size is $N \times N$. Then, $x_p$ and $y_p$ can be expressed as

$$\{x_p, y_p\} \equiv \frac{2p-N-1}{N}, \qquad 1 \le p \le N. \tag{3}$$

The approximation $\hat{f}_p$ of $F$ at samples $(x_p, y_p)$ is given by the linear system

$$\hat{f}_p(x_p,y_p) \approx \sum_{k=0}^{K_x-1}{}' \sum_{r=0}^{K_y-1}{}' c_{k,r} T_k(x_p) T_r(y_p). \tag{4}$$

In matrix notation, this system is of the form

$$\hat{\boldsymbol{f}} \approx \boldsymbol{T}\boldsymbol{c} \tag{5}$$

where $\boldsymbol{T} = T_k T_r$. From (5) we may estimate $\boldsymbol{c}$ with the Moore-Penrose pseudo-inverse of $\boldsymbol{T}$, which provides the least-squares solution of smallest norm of the linear system [9]. The estimation $\hat{\boldsymbol{c}}$ of coefficients $\boldsymbol{c}$ in (5) is given by

$$\hat{\boldsymbol{c}} \equiv \boldsymbol{T}^{\dagger}\hat{\boldsymbol{f}}, \tag{6}$$

where $\boldsymbol{T}^{\dagger}$ is the pseudo-inverse of $\boldsymbol{T}$. For instance, if we take $(x_p, y_p) = (0,0)$, the estimate of $F(0,0)$, is

$$\hat{F}(0,0) = \hat{f}_p(0,0) \equiv \boldsymbol{T}(0,0)^T \boldsymbol{T}^{\dagger}\hat{\boldsymbol{f}} \tag{7}$$

and the kernel value at the central position is $\boldsymbol{T}(0,0)^T\boldsymbol{T}^{\dagger}$. The remaining values of the estimate of $F$ are straightforward, as $F$ was assumed to be sampled in a $N \times N$ uniform grid. Consequently, the convolution kernel of size $N \times N$ is

$$[\boldsymbol{K}_{ch}]_{\alpha+1,\beta+1} \equiv [\boldsymbol{T}(0,0)^T\boldsymbol{T}^{\dagger}]_{N-p-1,N-p-1}, \tag{8}$$

where $\alpha = 0,\, 1, \ldots,\, N-1$ and $\beta = 0,\, 1, \ldots,\, N-1$.

### 2.2. Unbiased Coherence Estimation

Coherence $\gamma$ quantifies the degree of correlation between the two SAR images combined $\boldsymbol{S}_1$ and $\boldsymbol{S}_2$, and it provides a direct indicator of the phase quality. Its estimator is

$$\gamma = \frac{|E\{\boldsymbol{S}_1\boldsymbol{S}_2^*\}|}{\sqrt{|E\{\boldsymbol{S}_1\boldsymbol{S}_1^*\}| \cdot |E\{\boldsymbol{S}_2\boldsymbol{S}_2^*\}|}} \tag{9}$$

where $E\{\}$ corresponds to a spatial average inside an estimation window.

Strong surface deformation caused by geological activities is observed in the differential phase image as dense fringe areas corresponding to the terrain motion. The presence of these fringes affects directly the correlation values [10]. Consequently, the effect of the surface deformation must be compensated in order to have unbiased estimations of the coherence. For doing so, a maximum likelihood estimation is applied to the interferogram in order to remove the dominant fringe frequencies corresponding to the deformation. In practice, the estimation is performed inside a (2P+1)×(2Q+1) window:

$$\{\hat{f}_x, \hat{f}_y\} = \max_{f_x, f_y} \left( \left| \sum_{x=p_0-P}^{p_0+P} \sum_{y=q_0-Q}^{q_0+Q} \boldsymbol{Z}_{p,q} e^{-2\pi j(f_x p + f_y q)} \right| \right) \tag{10}$$

where $\{f_x, f_y\}$ are the local two-dimensional frequencies at indexes $(p,q)$ and $\boldsymbol{Z}_{p,q} = e^{2\pi j(f_x p + f_y q)}$ is the phase of the complex differential interferogram. The slope-compensated phase values $\hat{\boldsymbol{Z}}$ at pixels $(p,\, q)$ are then expressed as

$$\hat{\boldsymbol{Z}}_{p,q} = z_{p,q} e^{-2\pi j[(\hat{f}_x p + \hat{f}_y q) - \hat{\theta}_0]} \tag{11}$$

where $\hat{\theta}_0$ is the phase at estimated $\{\hat{f}_x, \hat{f}_y\}$ main frequencies.

### 2.3. Iterative Filtering

In this work, an iterative filter for phase denoising is proposed. The original interferogram is filtered multiple times with filtering windows of decreasing size. In the first iterations, larger windows are employed as they provide a higher noise suppression. For instance, an initial $256 \times 256$ window can be used. At each iteration, the window size is reduced by half until a minimum size is reached, for instance, a $8 \times 8$ window.

In addition, the subtraction of the local phase gradient by means of (10) and (11) is employed both for coherence estimation and prior to the filtering operation. The removal of the main frequencies causes an increase in the correlation, so the remaining phase values constitute a direct measure of the noise. Moreover, as the local fringes are removed from the original signal, only the spectrum of the remaining noise is filtered, so the information related to the deformation is better preserved.

Concerning the formulation of the proposed method, it is similar to the conventional Goldstein filter. At the each iteration, the interferogram is segmented into patches of the corresponding window size. An overlap between patches is fixed in both dimensions to avoid discontinuities at the edges. The size of the filtering kernel is adaptive, so it varies in each iteration of the algorithm. Its size is fixed to the square root of the size of the filtering window in each iteration. After removing the local phase ramp, the flattened interferogram is convolved (smoothed) with the kernel in the spatial domain. Then, the spectrum of the original interferogram $\boldsymbol{S}_{or}$ is weighted with the spectrum of the smoothed block $\boldsymbol{S}_m$ , and the spectrum of the filtered interferogram $\boldsymbol{S}_f$ is obtained by means of

$$[\boldsymbol{S}_f] = |[\boldsymbol{S}_m]|^{\alpha} \bullet [\boldsymbol{S}_{or}] \tag{12}$$

where $\alpha = 1 - \bar{\gamma}$, being $\bar{\gamma}$ the mean coherence of the effective filtering window (non-overlapped area between adjacent windows). Notice that, in our method, the values of $\alpha$ will be smaller than in other filters, but the iterative filtering will progressively remove the phase noise. The last step consists in adding the estimated frequencies to the filtered phase.

## 3. RESULTS

### 3.1. Simulated data

To validate the proposed method, it went through a test with a simulated interferogram in which noise is added to the original phase values. The standard deviation of the phase noise added is 1.5 rad. The quality of the filter is assessed by the number of residues and the Mean Square Error (MSE)

$$MSE = E\left\{|arg(e^{j(\boldsymbol{\phi_F} - \boldsymbol{\phi_{ideal}})})|^2\right\} \tag{13}$$

where $\boldsymbol{\phi_F}$ is the filtered phase and $\boldsymbol{\phi_{ideal}}$ is the noise-free phase. The performance of our method is compared with the one of already-existing filters, such as the widely-used adaptive Goldstein filter and the RASF (which also follows an iterative strategy).

All the filtering parameters are summarized in Table 1. In order to correctly compare all methods, the same parameters have been used when possible (when they are common).

**Table 1**: Filter parameters.

| **Filter type** | Window size | Coherence estimation | Smoothing operator |
|---|---|---|---|
| Modified Goldstein | 256×256 | 5×5 | Gaussian kernel 7×7 |
| RASF | 256×256 to 8×8 | 5×5 | Gaussian kernel 7×7 |
| Proposed method | 256×256 to 8×8 | 5×5 | Adaptive kernel based on Chebyshev functions. The polynomial order is 15. |

In Fig. 1, we show the filtered phases of the simulated scene. As it can be observed, the Adaptive-Goldstein filter provides good results in fringe preservation but noise reduction in wide areas is limited. Concerning the RASF, it shows good results it noise suppression, but the phase is clearly over-filtered in the dense fringe area of the central part of the interferogram. However, our proposed method clearly exhibits the best visual results in noise reduction in wide areas along with fringe preservation.

Finally, the quantitative results are summarized in Table 2. Among the different filters, our proposed method provides the best results in terms of residues and MSE.

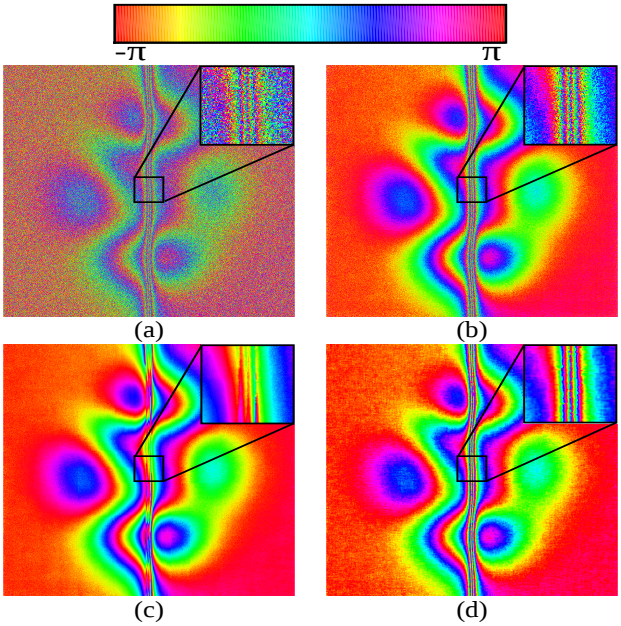


**Fig. 1**: Filtering results of the simulated scene with different methods: (a) Original noisy phase. (b) Adaptive Goldstein filter. (c) RASF. (d) Proposed method.

**Table 2**: Evaluation of different filters for simulated data set.

| **Interferogram** | Residue number | Improvement | MSE |
|---|---|---|---|
| Original phase | 217540 | – | 1.784 |
| Adaptive Goldstein | 5306 | 97.56% | 0.175 |
| RASF | 58 | 99.97% | 0.097 |
| **Our method** | **29** | **99.99%** | **0.026** |

### 3.2. Real data

In this section, we evaluate each filter with a real interferogram corresponding to the August 2016 Central Italy earthquake. Images were acquired in dates 2016-08-20 and 2016-20-08 by the Sentinel-1 satellite in Interferometric Wide swath (IW) mode. The near range and far range incidence angles are 36.05° and 41.96°, respectively. The polarimetric channel is VV. All the filtering parameters are the same as in the previous simulation. The resulting differential phases

are shown in Fig. 2 and the quantitative filtering results are summarized in Table 3.

As it can be observed in Fig. 2(a), the original phase presents a high level of noise and the number of residues is very large. Only both iterative filters are able to greatly suppress the noise, whereas noise suppression provided by the conventional Adaptive Goldstein filter is limited in very noisy areas. The number of remaining residues is still large with this method, while both iterative filters can reduce the number of residues to a greater extent. However, our proposed method shows a significantly cleaner and smoother phase, as shown in Fig. 2(d) and the cancellation of residues is almost total.

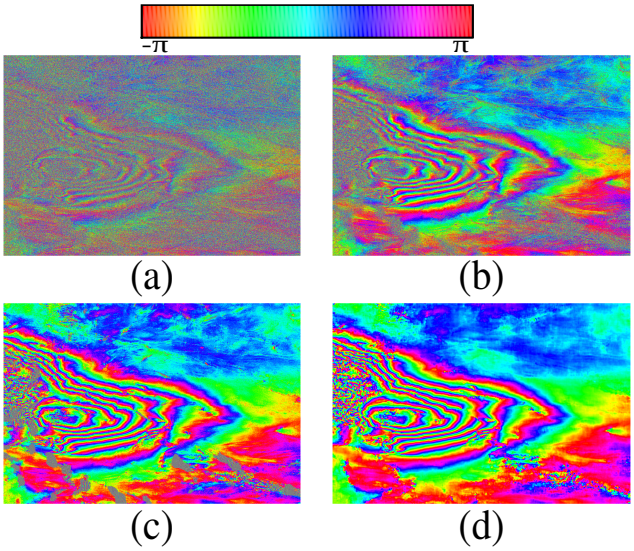


**Fig. 2**: Sentinel-1 interferogram filtered with different methods: (a) Original noisy phase. (b) Adaptive-Goldstein filter. (c) RASF. (d) Proposed method.

**Table 3**: Evaluation of different filters for Sentinel-1 data set.

| **Interferogram** | Residue number | Improvement |
|---|---|---|
| Original phase | 2074574 | – |
| Adaptive Goldstein | 787238 | 62.05% |
| RASF | 33006 | 98.41% |
| **Our method** | **1302** | **99.94%** |

## 4. CONCLUSION

An improved method for noise suppression in interferometric SAR images has been presented in this work. The combination of an iterative filtering with an specific smoothing kernel based on Chebyshev polynomials functions, has shown to progressively denoise the original phase image while preserving the original phase structure. The method is able to recover useful measurements even in very noisy areas. The proposed filter outperforms different already-existing filters, including the Goldstein filter and the RASF, which is also iterative. More details of the proposed filtering method can be found in [11].

## 5. REFERENCES


[1] D. Massonnet *et al.*, "The displacement field of the Landers earthquake mapped by radar interferometry," *Nature*, vol. 364, pp. 138–142, July 1993.

[2] P. Berardino, G. Fornaro, R. Lanari, and E. Sansosti, "A new algorithm for surface deformation monitoring based on small baseline differential SAR interferograms," *IEEE Trans. Geosci. Remote Sensing*, vol. 40, no. 11, pp. 2375–2383, Nov 2002.

[3] A. Hooper, H. Zebker, P. Segall, and B. Kampes, "A new method for measuring deformation on volcanoes and other natural terrains using InSAR persistent scatterers," *Geophysical Research Letters*, vol. 31, no. 23, 2004, l23611.

[4] H. A. Zebker and J. Villasenor, "Decorrelation in interferometric radar echoes," *IEEE Trans. Geosci. Remote Sensing*, vol. 30, no. 5, pp. 950–959, Sept 1992.

[5] R. M. Goldstein and C. Werner, "Radar interferogram filtering for geophysical applications," *Geophysical Research Letters*, vol. 25, no. 21, pp. 4035–4038, 1998.

[6] I. Baran *et al.*, "A modification to the Goldstein radar interferogram filter," *IEEE Trans. Geosci. Remote Sensing*, vol. 41, no. 9, pp. 2114–2118, Sept 2003.

[7] Z. Suo *et al.*, "Improved InSAR phase noise filter in frequency domain," *IEEE Trans. Geosci. Remote Sensing*, vol. 54, no. 2, pp. 1185–1195, Feb 2016.

[8] P. J. Gonzalez, "RSF: A robust non-parametric phase filtering method for automatic processing of Sentinel-1 interferograms," in *Proceedings of FRINGE15*, Frascati, Italy, Mar 2015.

[9] J. C. Mason and D. C. Handscomb, *Chebyshev Polynomials*. CRC Press LLC, 2003.

[10] H. A. Zebker and K. Chen, "Accurate estimation of correlation in InSAR observations," *IEEE Geoscience and Remote Sensing Letters*, vol. 2, no. 2, pp. 124–127, April 2005.

[11] A. Mestre-Quereda, J. M. Lopez-Sanchez, J. Selva, and P. J. Gonzalez, "An improved phase filter for differential SAR interferometry based on an iterative method," *IEEE Trans. Geosci. Remote Sensing*. [Online]. Available: http://dx.doi.org/10.1109/TGRS.2018.2820725